16th World Conference on Earthquake, 16WCEE 2017

Santiago Chile, January 9th to 13th 2017

Paper N° 312

Registration Code: S-F1461904603

POST EARTHQUAKE EVALUATION OF AXIAL FORCES AND BOUNDARY CONDITIONS FOR HIGH-TENSION BARS

S. Li[(1)], I. Josa[(2)] and E.Cavero[(3)]

[(1)] *Associate Professor, Tongji University, Lszh@tongji.edu.cn*
[(2)] *Master student, Tongji University and Universitat Politècnica de Catalunya, irene@cullere.net*
[(3)] *Master student, Tongji University and Universitat Politècnica de Catalunya, enrique.cavlap@gmail.com*

Abstract

High-tension bars or cables, such as diagonal braces of a truss, cables of a bridge, struts of a space structure, tie-bars of an arch, various anchorage cable and rods, usually play an important role in a civil structure. Identification of axial forces in these members is critical to post earthquake damage assessment of the structure. In view of the increasing uncertainty in boundary conditions due to seismic damage, two analytical methods assuming that the member is an Euler-Bernoulli beam or a Timoshenko beam are examined for rapid estimation of axial forces in high-tension bars based on dynamic testing. Bending stiffness effects are taken into account. Using the dynamic measurements from five or more sensors, the methods are able to identify the axial force in the bar and to determine the damage degree of the supports at two ends.

Numerical studies based on finite element methods are conducted for a single beam member, considering different parameters with regard to the effect of bending stiffness, slenderness ratio and boundary condition, to compare the effectiveness of the two methods in a wide range of situations. It turns out that the two methods are more suitable for the lower values of the non-dimensional parameter ξ for bending stiffness. When ξ<30, both methods can achieve good estimation with high accuracy. On the other hand, the estimation error of the Euler beam based method rapidly increases with the decrease of the slenderness ratio till the value of 20. The Timoshenko beam based method, comparatively, is quite steady and completely independent of this parameter.

A more complex externally prestressed structure is then simulated to investigate the feasibility of the methods by using both global and local modes. It is validated that all the cable tension estimations have been achieved with high accuracy. The estimation errors are less than 5%.

Laboratory experiments are carried out to validate the applicability and accuracy of the two methods. A steel bar is fixed at both ends onto the loading device and loaded increasingly by uniaxial tension. Using the frequencies and mode shapes identified by modal tests, the axial forces as well as the boundary conditions of the specimen are determined based on the two methods. It has been validated that most identified axial forces achieve a satisfied accuracy with a relative error below 10%. All the identified boundary stiffness approaches infinite, consistent with the actual fixed end.

Keywords: post-earthquake evaluation, axial force, boundary condition, dynamic testing, high-tension bar

1. Introduction

Modern advances in material, analysis, and construction technology have resulted in increasing number of high tension bars in civil structures such as bridges, beam string structures, trusses, spatial grid structures, and cable-membrane systems. Since they are crucial components for the overall structure in most cases, accurate measurement of cable tension force is strategic for safety evaluation and maintenance of the structures in service and even more important after earthquake.

Vibration based methods are amongst the most widely employed techniques for cable force identification owing to their simplicity, speed and economy. Depending on whether sag-extensibility and bending stiffness are taken into account, these methods may be classified into four categories, including the classic taut string theory that neglects both effects, the approach based on modern cable theory that accounts for sag-extensibility without bending stiffness, the technique that considers bending stiffness but neglects sag-extensibility, and the last category that takes the two effects into account.

The classic taut string theory was first used to determine cable forces by using the basic mode of vibration by hand and employing a simple relation between the fundamental frequency and the tensile force. The second technique mainly focuses on slender or high-tensioned cables and involves solving nonlinear characteristic equations by the trial-and-error method. Irvine [1], one of the most important authors in this field, was the first to show how the symmetric in-plane modes were heavily dependent on a parameter which allowed for the effects of cable geometry and elasticity.Due to their correspondence with many practical situations, the last two categories that involve bending stiffness effects have always attracted extensive attention. On the basis of single mode natural frequencies, some practical formulas were proposed by introducing a non-dimensional parameter ξ for bending stiffness [2]. While these methods are simple and speedy, they have limitations to the members which are not slender or not sufficiently tensioned since the applicable range of the formulae depends on the value of ξ. It was not until Zui [3] that someone dealt with those problems presenting new formulae exclusively of use for small values of ξ. Mehrabi and Tabatabai [4] were also the first to introduce a unified finite difference approach taking into account the combined effects of all important parameters involved including tension, sag-extensibility, bending stiffness, end conditions, variable cross sections, and intermediate springs or dampers. Even though the formulation was computationally efficient, these formulas relied on the assumption that the ends of the beam member are hinged or fixed but, in engineering practice, boundary conditions are more complex than that. To account for the influence of boundary rotational stiffness, Lagomarsino and Calderini [5] addressed the problem of identifying the tensile axial force of metallic tie-rods in masonry arches and vaults by using the first three modal frequencies of the tie-rod. Tullini and Laudiero [6] proposed a method based on one natural frequency and the corresponding modal displacements at three points determining the axial force as well as the boundary rotational stiffness under the condition of infinite translational stiffnesses at the beam ends.

It is worth noting that most of the aforementioned methods require not only the measured modal parameters but also additional information such as the effective vibration length of the beam member. However, such information, which affects the accuracy of the resulting force, is often not available in practice. Especially as the anchorage devices become complicated and uncertain after earthquake, the determination of the real vibration length and the boundary conditions is quite difficult. Two methods have recently been proposed solving this problem based on the dynamic measurements from at least five sensors by assuming that the member is an Euler-Bernoulli beam [7] or a Timoshenko beam [8].

Aiming to post earthquake damage assessment of a structure, two analytical methods recently presented by Li et al. [7] and Maes et al. [8] are examined for rapid estimation of axial forces and boundary stiffnesses in high-tension bars based on dynamic testing. Numerical studies for a single beam member are first conducted regarding different parameters defining the effect of bending stiffness and slenderness ratio to compare the effectiveness of the two methods in a wide range of situations. A more complex externally prestressed structure is then simulated to investigate the feasibility of the methods by using both global and local modes. Laboratory experiments are finally conducted to validate the applicability and accuracy of the two methods.

2. Theoretical formulation

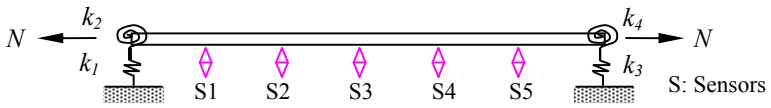

Fig. 1 –A beam member

This section examines theoretically the estimation of axial forces and boundary conditions for tension bars (as shown in Fig.1) through the vibration-based estimation from the data of five or more sensors. The transversal force and moment equilibrium for a free beam section are given, respectively, by:

$$\frac{\partial V(x,t)}{\partial x} + N\frac{\partial^2 v(x,t)}{\partial x^2} = \rho A\frac{\partial^2 v(x,t)}{\partial t^2} \tag{1}$$

$$V(x,t) + \frac{\partial M(x,t)}{\partial x} = \rho I\frac{\partial^2 \beta_z(x,t)}{\partial t^2} \tag{2}$$

Here $M(x, t)$ is the bending moment and $V(x, t)$ is the shear force, both defined along the deformed member coordinate system; N is the axial force, positive in tension; the transverse displacement of the centerline is $v(x, t)$ and $\beta_z(x, t)$ is the rotation of the beam cross-section. The position along the centerline x and the time t occur as independent variables. The area of cross section A, geometric moment of inertia I and material density ρ are assumed to be known. The axial force N and the boundary stiffness ($k_1 \sim k_4$) are unknowns to be identified by using the measurements of five sensors ($S_1 \sim S_5$).

2.1 The method based on Euler-Bernoulli beam theory

If an Euler-Bernoulli beam is considered [7], with the constant axial force N, the flexural stiffness EI and the mass per unit length m, then the equation of free vibration of the system can be written as

$$EI\frac{\partial^4 v(x,t)}{\partial x^4} + N\frac{\partial^2 v(x,t)}{\partial x^2} + \overline{m}\frac{\partial^2 v(x,t)}{\partial t^2} = 0 \tag{3}$$

A solution of this equation can be obtained by separation of variables as:

$$v(x,t) = \phi(x)Y(t) \tag{4}$$

It presents the free vibration motion with specific shape $\phi(x)$ and being time-dependent with an amplitude Y(t).

Substituting this expression in Eq.(3), it yields two ordinary differential equations

$$\ddot{Y}(t) + \omega^2 Y(t) = 0 \tag{5}$$

$$\phi^{iv}(x) + g^2\phi''(x) - \alpha^4\phi(x) = 0 \tag{6}$$

in which g^2 is given by

$$g^2 \equiv \frac{N}{EI} \tag{7}$$

The natural frequency and mode shape of the beam element can be obtained by

$$\omega^2 \equiv \frac{\alpha^4 EI}{\overline{m}} \tag{8}$$

$$\phi(x) = C_1\cos q_1 x + C_2\sin q_1 x + C_3\cosh q_2 x + C_4\sinh q_2 x \tag{9}$$

where C_1, C_2, C_3, C_4 are real constants; q_1, q_2 are written as:

$$q_1 \equiv \sqrt{\left(\alpha^4 + \frac{g^4}{4}\right)^{1/2} + \frac{g^2}{2}} \quad \text{and} \quad q_2 \equiv \sqrt{\left(\alpha^4 + \frac{g^4}{4}\right)^{1/2} - \frac{g^2}{2}} \tag{10}$$

For a given value of the frequency ω, the parameters q_1 and q_2 only depend on the axial force N according to Eq.(7) and Eq.(8).

2.2 The method based on Timoshenko beam theory

If the Timoshenko's beam theory is adopted [8], a partial differential equation can be obtained, containing the transverse displacement $v(x, t)$ as the only dependent variable:

$$EI\frac{\partial^4 v}{\partial x^4} + \frac{EIN}{k_y GA}\frac{\partial^4 v}{\partial x^4} - N\frac{\partial^2 v}{\partial x^2} - \frac{EI\rho}{k_y G}\frac{\partial^4 v}{\partial t^2 \partial x^2} - \rho I\frac{\partial^4 v}{\partial t^2 \partial x^2} - \frac{N\rho I}{k_y GA}\frac{\partial^4 v}{\partial t^2 \partial x^2} + \rho A\frac{\partial^2 v}{\partial t^2} + \frac{\rho^2 I}{k_y G}\frac{\partial^4 v}{\partial t^4} = 0 \tag{11}$$

where $k_y = A_s/A$ (called the Timoshenko shear coefficient), is a shear deformation coefficient depending on the geometry and G is the shear modulus of the material.This equation can be transformed to an ordinary differential equation if a separation of variables is performed and assuming that the transverse displacement $v(x, t)$ is harmonic at a frequency ω:

$$v(x,t) = \phi(x)\sin(\omega t) \tag{12}$$

It can be obtained by substituting Eq.(12) into Eq.(11):

$$a\frac{d^4\phi(x)}{dx^4} + b\frac{d^2\phi(x)}{dx^2} + c\phi(x) = 0 \tag{13}$$

with a, b and c defined as:

$$a = EI\left(1 + \frac{N}{k_y GA}\right) \tag{14}$$

$$b = -N + \frac{EI\rho\omega^2}{k_y G} + \rho I\omega^2 + \frac{N\rho I\omega^2}{k_y GA} \tag{15}$$

$$c = -\rho A\omega^2 + \frac{\rho^2 I\omega^4}{k_y G} \tag{16}$$

For a given value of the frequency ω, the parameters a, b and c only depend on the axial force N. The solution for Eq.(13) is given by:

$$\phi(x) = \sum_{k=1}^{4} C_k \exp(\beta_k x) \tag{17}$$

with

$$\beta_1 = \sqrt{\frac{-b+\sqrt{b^2-4ac}}{2a}},\ \beta_2 = -\sqrt{\frac{-b+\sqrt{b^2-4ac}}{2a}},\ \beta_3 = \sqrt{\frac{-b-\sqrt{b^2-4ac}}{2a}},\ \beta_4 = -\sqrt{\frac{-b-\sqrt{b^2-4ac}}{2a}} \tag{18}$$

2.3. Evaluation of axial forces and boundary conditions.

The major concern is to identify the axial force and boundary conditions based on the known structural parameters and the measured modal information (ω, ϕ) obtained from sensors distributed along the beam. The ratio of modal displacements in any two points, e.g. point i and j, can be calculated by:

$$\text{Euler beam:}\quad \lambda_{ij}=\frac{\phi_i}{\phi_j}=\frac{C_1\cos q_1x_i+C_2\sin q_1x_i+C_3\cosh q_2x_i+C_4\sinh q_2x_i}{C_1\cos q_1x_j+C_2\sin q_1x_j+C_3\cosh q_2x_j+C_4\sinh q_2x_j} \tag{19-1}$$

$$\text{Timoshenko beam:}\quad \lambda_{ij}=\frac{\phi_i}{\phi_j}=\frac{C_1e^{\beta_1x_i}+C_2e^{\beta_2x_i}+C_3e^{\beta_3x_i}+C_4e^{\beta_4x_i}}{C_1e^{\beta_1x_j}+C_2e^{\beta_2x_j}+C_3e^{\beta_3x_j}+C_4e^{\beta_4x_j}} \tag{19-2}$$

On the basis of four ratios of modal properties extracted from five sensors, characteristic equations can be constructed as:

$$\mathbf{S}_{4\times4}\cdot\begin{pmatrix}C_1 & C_2 & C_3 & C_4\end{pmatrix}'=0 \tag{20}$$

where [**S**] is the characteristic matrix. Its components are given according to Eq. (19) for acceleration, velocity or displacement dynamic measurements. Eq.(20) is a critical equation for the solution of the inverse problem in this study. As $[C_1 \quad C_2 \quad C_3 \quad C_4]'$ must have a non-zero solution, the determinant of the characteristic matrix has to be equal to zero:

$$|\mathbf{S}|=0 \tag{21}$$

from which the parameters (q_1, q_2) or (β_1, β_2 , β_3, β_4) as well as the axial force can be determined. The boundary stiffness can be then derived, as presented in Table 1.

Table 1 – Expressions for boundary stiffness

Stiffness	Euler beam	Timoshenko beam
k_1	$\frac{EI(-C_2q_1^3+C_4q_2^3)+N(C_2q_1+C_4q_2)}{C_1+C_3}$	$[EI(C_1\beta_1^3+C_2\beta_2^3+C_3\beta_3^3+C_4\beta_4^3)+N(C_1\beta_1+C_2\beta_2+C_3\beta_3+C_4\beta_4)]/(C_1+C_2+C_3+C_4)$
k_2	$\frac{EI(-C_1q_1^2+C_3q_2^2)}{C_2q_1+C_4q_2}$	$\frac{EI(C_1\beta_1^2+C_2\beta_2^2+C_3\beta_3^2+C_4\beta_4^2)}{C_1\beta_1+C_2\beta_2+C_3\beta_3+C_4\beta_4}$
k_3	$[EI(C_1q_1^3\sin q_1L-C_2q_1^3\cos q_1L+C_3q_2^3\sinh q_2L+C_4q_2^3\cosh q_2L)+N(-C_1q_1\sin q_1L+C_2q_1\cos q_1L+C_3q_2\sinh q_2L+C_4q_2\cosh q_2L]/(C_1\cos q_1L+C_2\sin q_1L+C_3\cosh q_2L+C_4\sinh q_2L)$	$[EI(C_1\beta_1^3\exp\beta_1L+C_2\beta_2^3\exp\beta_2L+C_3\beta_3^3\exp\beta_3L+C_4\beta_4^3\exp\beta_4L)+N(C_1\beta_1\exp\beta_1L+C_2\beta_2\exp\beta_2L+C_3\beta_3\exp\beta_3L+C_4\beta_4\exp\beta_4L)]/(C_1\exp\beta_1L+C_2\exp\beta_2L+C_3\exp\beta_3L+C_4\exp\beta_4L)$
k_4	$[EI(-C_1q_1^2\cos q_1L-C_2q_1^2\sin q_1L+C_3q_2^2\cosh q_2L+C_4q_2^2\sinh q_2L]/(-C_1q_1\sin q_1L+C_2q_1\cos q_1L+C_3q_2\sinh q_2L+C_4q_2\cosh q_2L)$	$[EI(C_1\beta_1^2\exp\beta_1L+C_2\beta_2^2\exp\beta_2L+C_3\beta_3^2\exp\beta_3L+C_4\beta_4^2\exp\beta_4L)]/(C_1\beta_1\exp\beta_1L+C_2\beta_2\exp\beta_2L+C_3\beta_3\exp\beta_3L+C_4\beta_4\exp\beta_4L)$

3. Numerical studies for a beam member

3.1 The effect of bending stiffness

Numerical studies using finite element (FE) method are conducted to verify the applicability of the methods. A critical non-dimensional parameter has been adopted to evaluate the effect of bending stiffness on free vibration of a beam-like structural member, which can be written as:

$$\xi=L\sqrt{\frac{N}{EI}} \tag{1}$$

A series of combination of the variables including the tension of the beam (N), its length (L), its elastic modulus (E) or its section area and therefore its moment of inertia (I) are considered to alter the value of ξ and evaluate the accuracy of the methods for the identification of the axial force.

The effect of bending stiffness is presented in Fig.2 (a). It can be seen that the two methods are more suitable for the lower values of ξ. When $\xi > 40$, both methods become increasingly unstable and consequently their errors are increasingly large; when $30 \leq \xi \leq 40$, the approach based on the Euler beam becomes numerically unstable whereas that on the Timoshenko beam achieves good accuracy; when $\xi < 30$, both methods have been verified to be effective with high accuracy.

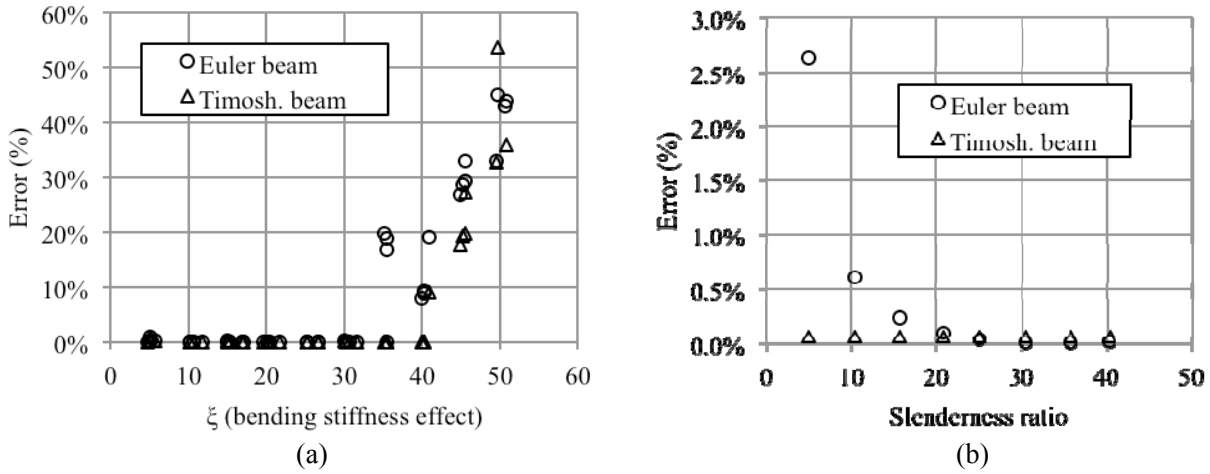

Fig. 2 –The effect of (a) bending stiffness and (b)slenderness ratio on the accuracy of the methods

3.2 The effect of slenderness ratio

To investigate the applicable conditions of the two methods, the next step is to focus on their main difference: shear and rotational inertia. A usual way to determine when these parameters become more or less relevant is by using the slenderness ratio, which is the ratio between the length and the width or the thickness of a structural element. When a beam member is very slender, the parameters such as the shear deformation or the rotational inertia can be neglected because their implications on the structural analysis are very small and therefore the formulation based on the Euler beam is valid for these cases.

Note that in order to maintain ξ constant (around 12), two different parameters have been adjusted at the same time: the length or the section that will change the slenderness ratio, and the tension that will compensate the alterations on the bending stiffness effects caused by the first change.

It stands clear from Fig.2 (b) that for the lower values of the slenderness ratio, the error of the method based on the Euler beam rapidly increases with the decrease of the slenderness ratio till the value of 20. On the other hand, the Timoshenko beam based method is quite steady regardless of the slenderness, showing that its approximation is completely independent of this parameter.

3.3 Identification of boundary conditions

Five beams with different boundary conditions have been investigated to verify the application of the proposed method for identifying the boundary stiffness. As shown in Table 2, all the parameters except the boundary stiffenesses (k1～k4) are same for the beams. The sensor placement as shown in Fig. 1 is employed. Using the first-order frequency and modal displacements, axial forces and boundary stiffness are finally determined.

Table 2 –Numerical cases for the beams with different boundary conditions

Cases	k_1(N/m)	k_2(Nm/rad)	k_3(N/m)	k_4(Nm/rad)	a(m)	b(m)	L(m)	E(N/m^2)	ρ(kg/m^3)	N(kN)
C1	∞	∞	∞	∞	0.08	0.012	0.72	2.10E11	7860	5
C2	∞	0	∞	0						
C3	∞	1000	∞	1000						
C4	∞	0	2000	0						
C5	∞	1000	2000	1000						

It can be found from Table 3 that the axial forces and the boundary stiffness identified by the two methods are all achieved with high accuracy. Note that C3-C5 are in an intermediate state between C1 (fixed-fixed beam) and C2 (simple beam). The good estimations verify a significant ascendancy of the methods by comparing with the traditional techniques which first assume the boundary conditions to be fixed or hinged and then identify axial forces directly based on the measured natural frequencies.

Table 3 –Identified axial forces and boundary conditions

Case		1	2	3	4	5
Euler beam	N_{id} (kN)	5.000	5.000	5.000	5.001	5.001
	k_1 (N/m)	1.04E+11	4.39E+12	5.07E+12	7.20E+12	2.10E+12
	k_2 (Nm/rad)	1.06E+12	-0.01	999.99	0	1000
	k_3 (N/m)	1.04E+14	4.39E+12	5.07E+12	1998.9	1998.86
	k_4 (Nm/rad)	2.23E+11	-0.02	999.97	0.05	1000.06
Timoshenko beam	N_{id} (kN)	5.000	5.001	5.000	5.000	5.002
	k_1 (N/m)	1.21E+11	1.17E+12	2.30E+12	4.15E+12	3.21E+12
	k_2 (Nm/rad)	2.06E+12	0.08	999.11	0.7	1002
	k_3 (N/m)	2.07E+13	1.13E+12	3.02E+12	1999.4	1999.1
	k_4 (Nm/rad)	1.17E+12	0.02	998.89	0.5	999.51

4. Numerical studies for a structure

To evaluate the accuracy of the two methods applied to more complex structures, an actual externally prestressed structure as shown in Fig.3 is investigated. The floor is a typical beam string structure (BSS), using bars connecting cables and concrete floor. A FE model is built up for this actual structure. Cables are modeled using 3-D spar elements while the concrete floor is defined by 3-D linear finite strain beam elements. The material and the geometric properties of the structures are listed in Table 4.

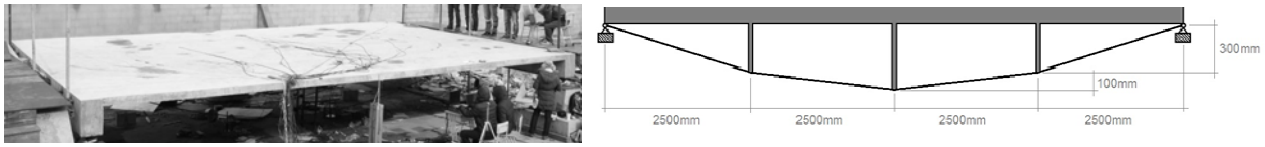

Fig. 3 –A cable-supported floor

Table 4 – Properties of the simulated structure

Concrete components		Cable				
E(N/m^2)	ρ(kg/m^3)	R(m)	N(kN)	E(N/m^2)	ρ(kg/m^3)	ξ
32E9	2300	0.0075	22.4	1.95E11	1101	12

Based on modal analysis, the first six frequencies and mode shapes of the structure are calculated and plotted in Fig.4. It can be seen that the first two are global modes for the full structure while the rest four are local modes for the cables. Using the calculated modal parameters, the axial forces can be identified by the two methods and compared with the set cable tension of 22.4kN. It can be found from Table 5 that all the cable tension estimations are achieved with high accuracy, either by using the global or local modes. The estimation errors are less than 5%.

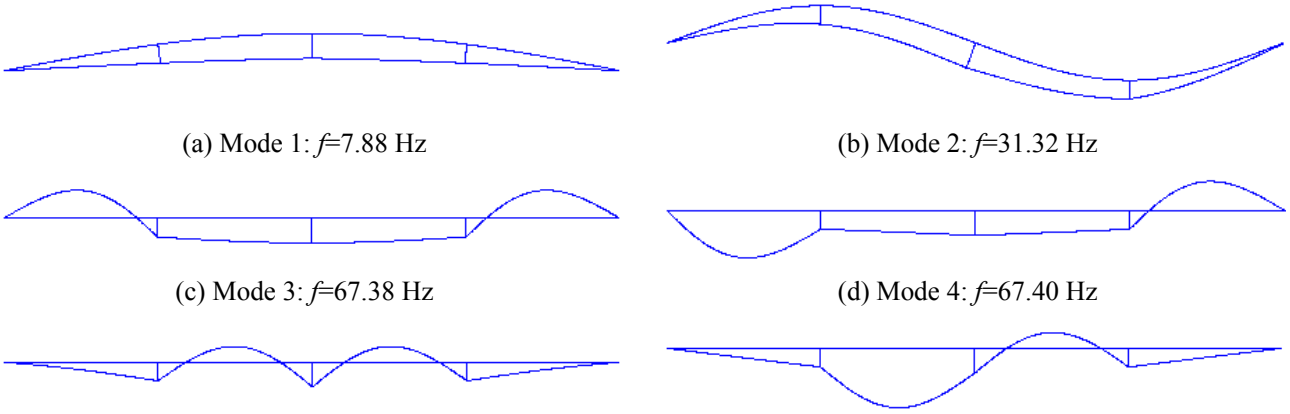

(a) Mode 1: f=7.88 Hz (b) Mode 2: f=31.32 Hz

(c) Mode 3: f=67.38 Hz (d) Mode 4: f=67.40 Hz

(e) Mode 5: f=67.83 Hz (f) Mode 6: f=67.83 Hz

Fig. 4 – Frequencies and mode shapes of the structure

Table 5 – Cable tension estimation of the cable-supported floor

Modes	1	2	3	4	5	6
	Global	Global	Local	Local	Local	Local
Euler beam	0.23%	1.92%	3.47%	3.46%	3.51%	3.51%
Timoshenko beam	0.23%	1.92%	3.46%	3.45%	3.51%	3.51%

5. Experimental investigation

Laboratory tests [7] have been carried out for a steel bar with 0.72m length and a rectangular cross section of 35mm×5mm. The specimen is fixed at both ends onto the loading device, i.e. k_1=k_2=k_3=k_4=∞, and loaded increasingly by uniaxial tension. Six cases are considered from 5kN to 30kN. Five accelerometers (0.1V/g, 1.5g mass) are installed onto its surface in an even distance along the length. For each case, single-point hammer impulsive excitation is applied and dynamic measurements from the five accelerometers are acquired at a sampling frequency of 2.5 kHz.

Using the frequencies and mode shapes identified by modal tests, the axial forces as well as the boundary conditions of the specimen are determined based on the above-mentioned two methods, as listed in Table 6. Most identified axial forces achieve a satisfied accuracy with a relative error below 10%. The estimations deviate a lot from the controlled load 5kN and the reason may be due to the low precision of loading device at a low loading level. All the identified boundary stiffness approaches infinite.

Table 6 – Experimental boundary conditions calculated with Euler-Bernoulli method

Cases	N (kN)	5	10	15	20	25	30
Euler beam	N_{id} (kN)	7.25	11.23	15.82	20.56	25.45	30.32
	Error (%)	45.0%	12.3%	5.5%	2.8%	1.8%	1.1%
	k_1 (N/m)	1.46E+11	4.00E+11	1.73E+12	1.11E+12	3.86E+11	2.06E+11
	k_2 (Nm/rad)	1.41E+11	1.63E+12	5.83E+11	7.80E+14	4.59E+11	4.68E+11
	k_3 (N/m)	3.62E+11	1.88E+12	1.51E+13	2.54E+11	1.49E+13	3.29E+12
	k_4 (Nm/rad)	3.82E+14	2.18E+13	1.44E+11	2.86E+13	1.35E+11	3.10E+11
Timoshenko beam	N_{id} (kN)	6.98	11.03	15.12	20.52	25.75	29.23
	Error (%)	39.6%	10.3%	0.8%	2.6%	3.0%	2.6%
	k_1 (N/m)	1.06E+12	3.01E+11	1.13E+12	2.01E+11	2.16E+12	2.35E+13
	k_2 (Nm/rad)	1.14E+11	1.50E+13	3.38E+11	5.08E+14	1.43E+11	3.57E+12
	k_3 (N/m)	3.62E+12	1.76E+12	1.15E+13	2.14E+11	2.50E+13	2.18E+12
	k_4 (Nm/rad)	2.32E+11	1.98E+13	2.74E+11	4.87E+13	1.45E+11	2.09E+11

6. Conclusions

Aiming to post earthquake damage assessment of a structure, two analytical methods assuming that the member is an Euler-Bernoulli beam or a Timoshenko beam are examined for rapid estimation of axial forces in high-tension bars based on dynamic testing. Bending stiffness effects are taken into account. Using the dynamic measurements from five or more sensors, the methods are able to identify the axial force in the bar and to determine the damage degree of the supports at two ends.

Numerical studies based on finite element methods for a single beam member verify that the two methods are more suitable for the lower values of the non-dimensional parameter ξ for bending stiffness. When $\xi > 40$, both methods become increasingly unstable and consequently their errors are increasingly large; when $30 \leq \xi \leq 40$, the approach based on the Euler beam becomes numerically unstable whereas that on the Timoshenko beam achieves good accuracy; when $\xi < 30$, both methods have been verified to be effective with high accuracy. On the other hand, the estimation error of the Euler beam based method rapidly increases as the slenderness ratio is less than the value of 20. The Timoshenko beam based method, comparatively, is quite steady and completely independent of this parameter.

Numerical simulations for an external prestressed structure verify the applicability of the two methods either by using the global or local modes. All the cable tension estimations are achieved with high accuracy. The estimation errors are less than 5%.

Laboratory experiments on a steel bar are carried out to validate the applicability and accuracy of the two methods. It has been validated that most identified axial forces achieve a satisfied accuracy with a relative error below 10%. All the identified boundary stiffness approaches infinite, consistent with the actual fixed end.

4. Acknowledgements

The authors are grateful to the Key Projects in the National Science & Technology Pillar Program (Grant No. 2013BAG19B00-02-04) for the financial support of this research work.

5. Copyrights

6. References

[1] M. Irvine (1978): Free vibrations of inclined cables. *Journal of the Structural Division*, *ASCE*, **104** (2), 343–347.

[2] T.Shimada, K. Kimoto and S. Narui (1989): Study on estimating tension of tied hanger rope of suspension bridge by vibration method. *Proc. Japan Society of Civil Engineers*, **404**(I-11), 455-458.

[3] H. Zui, T. Shinke, Y. Namita (1996): Practical formulas for estimation of cable tension by vibration method. *Journal of Structural Engineering, ASCE*, **122**, 651–656.

[4] A. B. Mehrabi, H. Tabatabai (1998): Unified finite difference formulation for free vibration of cables. *Journal of Structural Engineering, ASCE*, **124**, 1313–1322.

[5] S. Lagomarsino, C. Calderini (2005): The dynamical identification of the tensile force in ancient tie-rods. *Engineering Structures*, **27** (6), 846–856.

[6] N. Tullini, F. Laudiero (2008): Dynamic identification of beam axial loads using one flexural mode shape. *Journal of Sound and Vibration*, **318**, 131–147.

[7] S. Li, E. Reynders, K. Maes, G. De Roeck (2013): Vibration-based estimation of axial force for a beam member with uncertain boundary conditions. *Journal of Sound and Vibration*, **332** (2), 795-806.

[8] K. Maes, J. Peeters, E. Reynders, G. Lombaert, G. De Roeck (2013): Identification of axial forces in beam members by local vibration measurements. *Journal of Sound and Vibration*, **332** (10), 5417-5432.